CHEMISTRY
A EUROPEAN JOURNAL

ChemPubSoc
Europe

DOI: 10.1002/chem.201202492

Origin of the Magnetic Anisotropy in Heptacoordinate Ni^{II} and Co^{II} Complexes

Renaud Ruamps,[a] Luke J. Batchelor,[b] Rémi Maurice,[a, c, d] Nayanmoni Gogoi,[e, f] Pablo Jiménez-Lozano,[d] Nathalie Guihéry,*[a] Coen de Graaf,[d, g] Anne-Laure Barra,[h] Jean-Pascal Sutter,[e, f] and Talal Mallah*[b]

Abstract: The nature and magnitude of the magnetic anisotropy of heptacoordinate mononuclear Ni^{II} and Co^{II} complexes were investigated by a combination of experiment and ab initio calculations. The zero-field splitting (ZFS) parameters D of $[Ni(H_2DAPBH)(H_2O)_2](NO_3)_2{\cdot}2H_2O$ (**1**) and $[Co(H_2DAPBH)(H_2O)(NO_3)](NO_3)$ (**2**; H_2DAPBH = 2,6-diacetylpyridine bis(benzoyl hydrazone)] were determined by means of magnetization measurements and high-field high-frequency EPR spectroscopy. The negative D value, and hence an easy axis of magnetization, found for the Ni^{II} complex indicates stabilization of the highest M_S value of the $S=1$ ground spin state, while a large and positive D value, and hence an easy plane of magnetization, found for Co^{II} indicates stabilization of the $M_S=\pm1/2$ sublevels of the $S=3/2$ spin state. Ab initio calculations were performed to rationalize the magnitude and the sign of D, by elucidating the chemical parameters that govern the magnitude of the anisotropy in these complexes. The negative D value for the Ni^{II} complex is due largely to a first excited triplet state that is close in energy to the ground state. This relatively small energy gap between the ground and the first excited state is the result of a small energy difference between the d_{xy} and $d_{x^2-y^2}$ orbitals owing to the pseudo-pentagonal-bipyramidal symmetry of the complex. For Co^{II}, all of the excited states contribute to a positive D value, which accounts for the large magnitude of the anisotropy for this complex.

Keywords: ab initio calculations · cobalt · heptacoordinate complexes · magnetic anisotropy · nickel

Introduction

One of the challenges in the field of molecular magnetism is the fundamental understanding of the origin of the magnetic anisotropy in mononuclear complexes that can be used as building blocks to prepare single-molecule magnets[1] and single-chain magnets.[2–4] One fruitful approach may be to combine synthetic chemistry and ab initio theoretical calculations. Such a strategy is valuable to chemists who appreciate simple rules that may direct their synthesis. Herein, we investigate the origin of the magnetic anisotropy of heptacoordinate Ni^{II} and Co^{II} complexes with pentagonal-bipyramidal geometry based on the pentadentate ligand 2,6-diacetylpyridine bis(benzoyl hydrazone), H_2DAPBH. The planarity of the pentadentate ligand ensures an axial structure and is expected to lead to large magnetic anisotropy.

[a] R. Ruamps, Dr. R. Maurice, Prof. N. Guihéry
Laboratoire de Chimie et Physique Quantiques
Université de Toulouse III
118, route de Narbonne
31062 Toulouse (France)
E-mail: nathalie.guihery@irsamc.ups-tlse.fr

[b] Dr. L. J. Batchelor, Prof. T. Mallah
Institut de Chimie Moléculaire et des Matériaux d'Orsay
CNRS, Université Paris Sud 11
91405 Orsay Cedex (France)
E-mail: talal.mallah@u-psud.fr

[c] Dr. R. Maurice
Zernike Institute for Advanced Materials
University of Groningen
9747 AG Groningen (The Netherlands)

[d] Dr. R. Maurice, P. Jiménez-Lozano, Prof. C. de Graaf
Departament de Química Física i Inorgànica
Universitat Rovira i Virgili
Marcel·li Domingo s/n
43007 Tarragona (Spain)

[e] Dr. N. Gogoi, Dr. J.-P. Sutter
CNRS; LCC (Laboratoire de Chimie de Coordination)
205, route de Narbonne
31077 Toulouse (France)

[f] Dr. N. Gogoi, Dr. J.-P. Sutter
Université de Toulouse; UPS, INPT; LCC
31077 Toulouse (France)

[g] Prof. C. de Graaf
Institució Catalana de Recerca i Estudis Avançats (ICREA)
Passeig Lluis Companys 23
08010, Barcelona (Spain)

[h] Dr. A.-L. Barra
Laboratoire National des Champs Magnétiques Intenses
UPR CNRS 3228, Université J. Fourier
25, avenue des Martyrs, B.P. 166
38042 Grenoble Cedex 9 (France)

Supporting information for this article is available on the WWW under http://dx.doi.org/10.1002/chem.201202492.

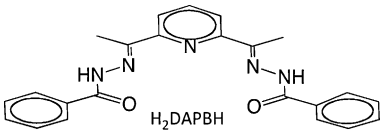

We have already combined experimental data and a semi-empirical theoretical approach to get insight into the magnetic anisotropy of hexacoordinate and pentacoordinate Ni^{II} complexes.[5–7] Theoretical studies have been already carried out on Ni^{II} and Co^{II} complexes[8–11] but, to the best of our knowledge, no reports on heptacoordinate Ni^{II} and Co^{II} complexes exist. This work aims to combine synthetic chemistry, physical studies, and ab initio calculations to unravel the effect of the different electronic parameters that govern the magnetic anisotropy in heptacoordinate complexes. Such insight aims to establish a correlation between magnetic anisotropy and parameters accessible to chemical manipulation. The approach focused here on Ni^{II} and Co^{II} heptacoordinate complexes is, of course, general and can eventually be applied to other metal ions with the same geometry and to other geometries, provided the symmetry remains very close to axial.

For mononuclear complexes having an orbitally nondegenerate electronic ground state and close-to-axial symmetry, the main contribution to magnetic anisotropy stems from the interaction between the ground and the excited electronic states coupled through the spin–orbit operator. These interactions lift the degeneracy of the $2S+1$ M_S components of the ground state, resulting in the so-called zero-field splitting (ZFS). The magnitude of the magnetic anisotropy (extent of ZFS) is therefore governed by the magnitude of the spin–orbit coupling (SOC) and by the energy difference between the ground and the excited electronic states. The smaller the energy difference between the ground and the excited states, the larger the interaction and thus the larger the magnetic anisotropy.

In this work, we investigated the magnetic anisotropy of complexes $[Ni(H_2DAPBH)(H_2O)_2](NO_3)_2{\cdot}2H_2O$ (**1**) and $[Co(H_2DAPBH)(H_2O)(NO_3)]NO_3$ (**2**) using magnetization measurements and EPR spectroscopy to estimate the ZFS parameters. Ab initio calculations were then carried out to rationalize the origin of the experimentally observed anisotropy and develop simple rules to tune the ZFS by small modifications of the complexes.

Results and Discussion

Synthesis and characterization: Complexes **1** and **2** were synthesized according to literature procedures[12,13] and characterized by mass spectrometry, elemental analysis, infrared spectroscopy, and a unit cell was collected to ensure that the structures were identical to those previously reported (see Supporting Information and Figure 1). Compound **1** contains a network of hydrogen bonds involving coordinated water and crystallization water molecules, the nitrate anions, and the oxygen atoms of the pentadentate ligand (Supporting Information Figure S1). Thermogravimetric analysis (TGA) of a freshly prepared microcrystalline powder of **1** showed steady water loss between 40 and 100 °C (Supporting Information Figure S2).

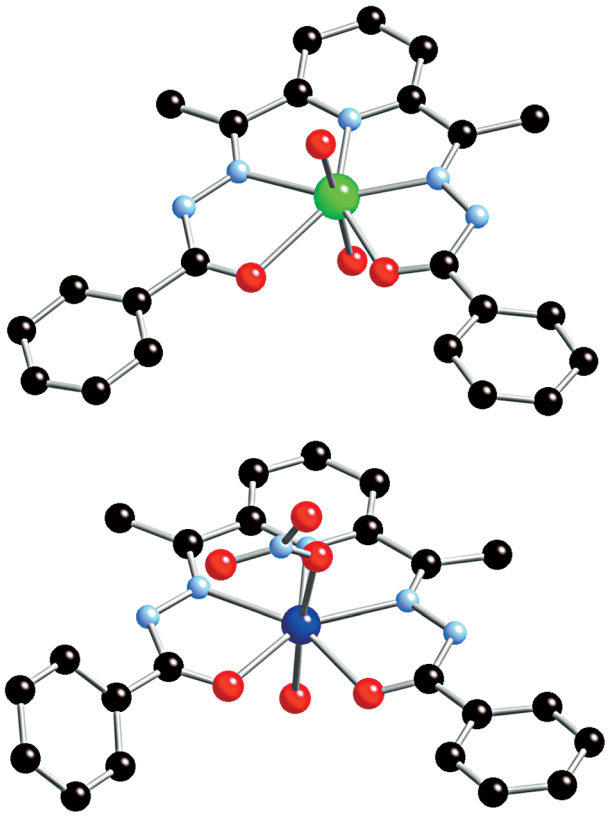

Figure 1. View of the molecular structures of **1** (top) and **2** (bottom).

Magnetic studies: Magnetization studies were carried out with a SQUID magnetometer (see Supporting Information). The temperature dependence of the magnetic susceptibility was measured at a fixed dc field of 0.1 T, and magnetization versus field was measured at 2, 4, and 6 K. Plotting $M=f(H/T)$ for **1** and **2** led to nonsuperimposable curves, which is a signature of the presence of a magnetic anisotropy (Figure 2). The data were fitted by using a home made software that diagonalizes the spin Hamiltonian with a g_{iso} value obtained from the $\chi_M T=f(T)$ curves (Supporting Information Figure S3) at high temperature to minimize the number of fitting parameters. The experimental data were fitted simultaneously for all temperatures by exact diagonalization of the energy matrices corresponding to the spin Hamiltonian $\mathbf{H}=\mu_B\mathbf{g}\cdot\mathbf{B}\cdot\mathbf{S}+D[\mathbf{S}_z^2-S(S+1)/3]+E[\mathbf{S}_x^2-\mathbf{S}_y^2]$, where D and E are the axial and rhombic anisotropy parameters, respectively) averaged over 120 orientations of the magnetic field. The best fits gave $D=-13.9\ cm^{-1}$, $E/D=0.11$, $g_{iso}=2.26$ for **1** and $D=31.0\ cm^{-1}$, $E/D=0$, $g_{iso}=2.22$ for **2**.

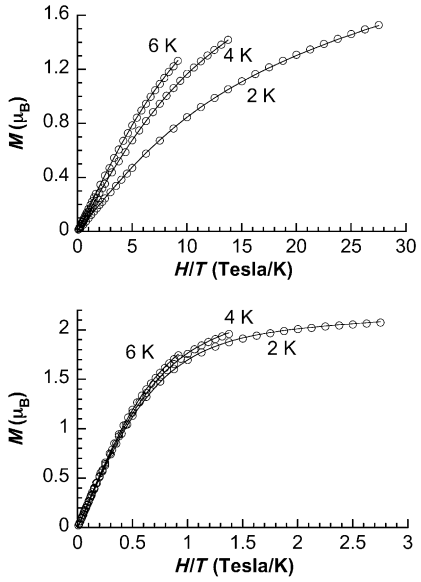

Figure 2. Reduced magnetization M versus H/T for **1** (top) and **2** (bottom) collected at 2, 4, and 6 K. Data were fitted by using homemade software described in text (solid lines); see text for parameters.

HF-HFEPR studies: We performed high-field high-frequency EPR (HF-HFEPR) studies on the two complexes. The HF-EPR powder spectra of pellet samples of complex **1** were measured at several frequencies ranging from 190 to 575 GHz. Notwithstanding the use of many different frequencies, a precise description of the magnetic anisotropy of the complex could not be obtained due to the observation of a large number of signals with respect to what is expected for a simple $S=1$ system. Hence, different samples were measured at an interval of several months. Even though the general shape of the spectra is the same, they exhibit differences in intensities, especially at 190 GHz for high field lines (Figure 3).

These two facts point towards the presence of several molecules with slightly different structural parameters within the powder, not detected by X-ray diffraction. Thus only estimates of the magnetic anisotropy parameters can be given. A first estimate comes from the spectra recorded at 380 GHz (Supporting Information Figure S4): the signal at a field very close to zero observed at this frequency indicates that an energy gap of about 12.6 cm^{-1} is present, which roughly corresponds to $|D+E|$ or $|D-E|$ for some of the molecules. The "zero-field" signal is, however, extremely large, so that slightly smaller $|D|$ values should also be present in the sample. In the spectra recorded at 190 and 285 GHz (Figure 3 and Supporting Information Figure S5), we can also recognize $\Delta M_S=1$ transitions originating from the ground M_S level and corresponding to x and y orientations of the molecules. At 190 GHz, there are four such lines (or rather groups of lines): one close to 5.5 T, another one close to 10.6 T, another one close to 13.5 T, and the last one close to 14.4 T. In the hypothesis that the lines at 5.5 and 13.5 T correspond to the x and y transitions from the same molecules, we obtain that $|E|\approx 1.6$ cm^{-1}, whereas the other two lines lead to $|E|\approx 3.3$ cm^{-1}. These values are in agreement with the large $|D|$ value obtained from magnetization measurements (-13.9 cm^{-1}) but do not allow us to establish a high-precision set of parameters.

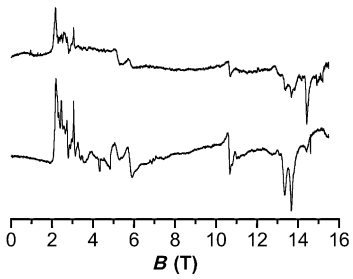

Figure 3. HF-HFEPR spectrum of **1** at 190 GHz and 5 K (bottom spectrum). The measurement was repeated several months later showing the change upon aging (top spectrum).

For Co^{II} (complex **2**), which has a half-integer spin, the D value is unfortunately too large for EPR to improve the magnetic anisotropy description as only effective spin 1/2 spectra are obtained up to the highest frequencies. Powder spectra were recorded in the frequency range from 190 to 460 GHz. All of them can be nicely reproduced by considering an $S=1/2$ spin with a rhombic effective g matrix, with $g_{eff1}=4.984$, $g_{eff2}=4.033$, and $g_{eff3}=1.996$ (Supporting Information Figure S6 and Figure 4). As the spectra at 460 GHz still only contain signals that originate from an $S=1/2$ spin, we can only deduce a lower bound for the axial anisotropy: $|D|>20$ cm^{-1}. Seemingly good fits can be obtained[14] by considering very different D values ($|D|>20$ cm^{-1}) for the $S=3/2$ spin and then adding rhombicity either on the g parameters or on the ZFS ones: if E is set to 0, then three g values are needed ($g_1=2.47$, $g_2=2.03$, and $g_3=1.99$); on the contrary, if there is no rhombicity in the g values ($g_1=g_2$), then good fits are obtained for $|E/D|=1/15$ with $g_1=g_2=2.26$ and $g_3=2.01$.

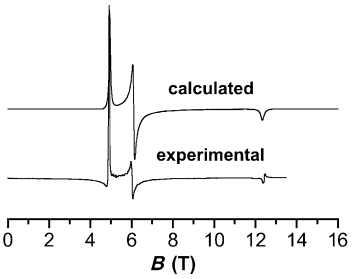

Figure 4. HF-HFEPR spectra of **2** at 345 GHz and 5 K; see text for parameters.

Theoretical calculations: To understand the difference in the sign and magnitude of D for **1** and **2**, we theoretically studied the two compounds using wave function based calculations and a procedure of extraction that has been successfully applied to other mononuclear and binuclear com-

plexes.[15–19] We first performed complete active space self-consistent field calculations (CASSCF), which account for nondynamic electron correlation and then used the *n*-electron valence second-order perturbation theory (NEVPT2) method to describe the dynamic correlation.[20] The CASSCF wave function contains all electronic configurations that can be constructed by distributing *n* electrons over the five 3d orbitals of Ni^{II} or Co^{II} ($n=8$ and 7 for **1** and **2**, respectively). Both spin–orbit and spin–spin couplings are calculated in the complete d^n manifold.[21,22] Two procedures of extraction of the *D* and *E* parameters were used which are associated with two different kinds of ab initio calculations.[23] Similar calculations have been performed on Mn^{III} complexes.[24] Calculations were performed with the ORCA code,[25] and the values were extracted using the effective Hamiltonian theory. Further computational details are given in the Supporting Information. The results for **1** and **2** are reported in Table 1.

Table 1. NEVPT2 values of *D* and *E* for **1** and **2** extracted with the effective Hamiltonian theory.

Complex	D [cm^{-1}]	E [cm^{-1}]
1	−16.83	1.15
2	35.42	2.20

The results of the calculations are in relatively good agreement in both magnitude and sign with the experimental data for **1** and **2**. In the following, we analyze these data by considering the individual contributions of the excited states to the overall *D* values. We aim to gain insight into the chemical parameters that govern the magnitude and the sign of the magnetic anisotropy. This is reasonably easy in the present case since due to the structural axial anisotropy of the complexes; the axis frame that diagonalizes the calculated $\overline{\overline{D}}$ tensors for **1** and **2** has the *z* axis along the bonds of the metal ion and the apical oxygen atoms. In addition, despite the almost pentagonal molecular plane that contains the *x* and *y* axes, the 3d orbitals are close to the pure d_{xy}, $d_{x^2-y^2}$, d_{z^2}, d_{xz}, and d_{yz} linear combinations of spherical harmonics obtained for an octahedral symmetry. For more strongly distorted complexes the expressions of the d orbitals become more complicated, which seriously hinders the derivation of simple rules to rationalize the magnetic anisotropy. Lifting of the degeneracy of the 3d orbitals for the two complexes is shown qualitatively in Figure 5. Because of the larger distortion in the pentagonal plane for Ni^{II} than for Co^{II}, the energy difference between the d_{xy} and the $d_{x^2-y^2}$ orbitals is larger for the former.

Inspection of the contributions of all excited states shows that only a few play a role in the magnitude and sign of the *D* parameters. Since the spin–spin coupling makes a smaller contribution to the anisotropy than the spin–orbit coupling, we rationalize the values and signs of *D* using only the spin–orbit operator $\Sigma\hat{\mathbf{l}}_i\cdot\hat{\mathbf{s}}_i$. This operator couples the ground state M_S components with those of the excited states and makes

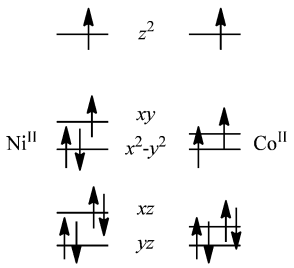

Figure 5. Orbital energy diagrams for **1** (left) and **2** (right).

the main contribution to the magnetic anisotropy. Concerning **1**, the interaction with the first three excited triplet states causes almost all of the magnetic anisotropy of the complex. To rationalize the nature and sign of the magnetic anisotropy, an estimate of the contribution of these excited states to *D* and *E* can be obtained by using perturbation theory. The perturbative calculated values are reported in Table 2.

Table 2. Main perturbative contributions of the triplet excited states to *D* and *E* for **1.**

	D [cm^{-1}]	E [cm^{-1}]
1st triplet	−66.2	0
2nd triplet	22.5	12.12
3rd triplet	23.2	−13.4

The wave function of the $M_S=1$ component of the triplet ground state is dominated by the $|d_{xy}d_{z^2}|$ determinant while the first triplet excited states is dominated by $|d_{x^2-y^2}d_{z^2}|$, corresponding to promotion of an electron from the $d_{x^2-y^2}$ to the d_{xy} orbital (see Figure 5). Since these two orbitals are both expressed as linear combinations of the d_{2+} and d_{2-} complex spherical harmonics, electron promotion does not imply changes in the m_l values. Hence, only the *z* component of the spin–orbit operator $\sum\hat{l}_{zi}\cdot\hat{s}_{zi}$ can couple the ground and the first excited triplet state. Because the coupling is restricted to the s_z component of the spin angular momentum, the spin–orbit operator only couples the M_S components of the ground and the excited state with the same value. The coupling between the $M_S=0$ components is zero by spin symmetry, while calculations show that the couplings between the $M_S=\pm1$ components are nonzero. This leads to stabilization of the $M_S=\pm1$ components of the ground triplet state, while the $M_S=0$ state remains unaffected. Therefore, the interaction between the ground state and the first excited triplet results in a negative contribution to *D*, as schematized in Figure 6 (top).

The second and third excited triplet state wave functions are linear combinations of determinants $|d_{xz}d_{xy}|$,$|d_{yz}d_{xy}|$, $|d_{xz}d_{z^2}|$, and $|d_{yz}d_{z^2}|$, corresponding to promotion of an electron from d_{xz} or d_{yz} to d_{xy} and d_{z^2}. These two excited triplet states couple to the ground state by the *x* and *y* components of spin–orbit operator $\sum\hat{l}_i^+\cdot\hat{s}_i^- + \hat{l}_i^-\cdot\hat{s}_i^+$ and not by the *z* component, at variance with the first excited state. As a con-

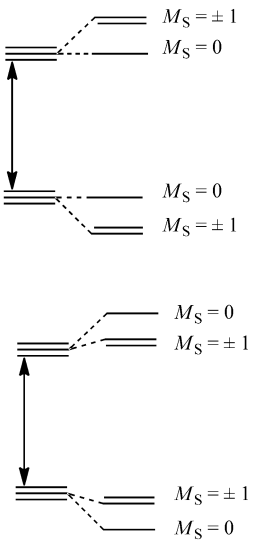

Figure 6. Interaction scheme between the ground and first triplet excited states through the z components of spin–orbit operator that couples M_S levels of the same values and stabilizes the $M_S = \pm 1$ components (top), and interaction between the ground and the second excited triplet states through the x and y components of the spin–orbit operator that couples states with different M_S values and stabilizes the $M_S = 0$ component (bottom).

sequence, the M_S components differing by ± 1 couple together, that is, $M_S = 0$ with $M_S = \pm 1$ and vice versa. The $M_S = 0$ component of the triplet ground state therefore benefits from two interactions (with the $M_S = 1$ and with the $M_S = -1$ components) of the excited states, while the two $M_S = \pm 1$ components of the ground state only benefit from the interaction with one component ($M_S = 0$) of the excited states. As a consequence, the $M_S = 0$ component of the ground triplet state is more stabilized than the $M_S = \pm 1$ components and the contribution of these two excited states to D is positive (Figure 6, bottom). However, the relative energy of the second and third excited triplets is higher than that of the first excited state, and hence this positive contribution is weaker and does not compensate the large negative contribution of the first excited triplet state. The resulting D value remains negative and is relatively large. Among the excited singlet states, six have a small but non-negligible contribution to D. Nevertheless, they all are of opposite value and almost completely compensate one another. The magnetic axes frame, which diagonalizes the computed $\overline{\overline{D}}$ tensor, has its easy axis of magnetization close to the $Ni(H_2O)_2$ bonds (Figure 7, top).

The very large positive D value of **2** results from three positive contributions (Table 3). The largest contributions arise from the interaction with two quartet and one doublet excited states. The ground-state wave function is dominated by the $|d_{xy}d_{x^2-y^2}d_{z^2}|$ determinant (see Figure 5), while the excited quartet states have a multideterminantal nature.

The determinants with the largest weights in these quartets have $|d_{xz}d_{xy}d_{x^2-y^2}|$ and $|d_{yz}d_{xy}d_{x^2-y^2}|$ character. Hence, their contribution to the axial D parameter is essentially due

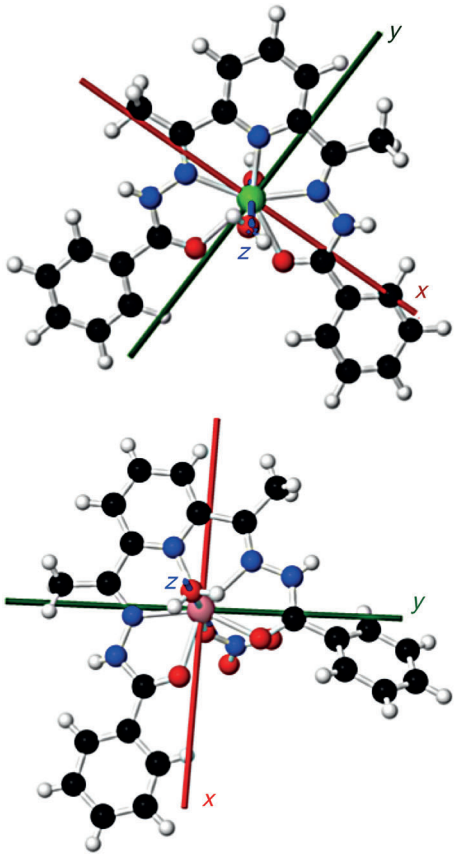

Figure 7. View of the magnetic axes obtained from ab initio calculations. For **1** (top), the magnetization is along z (negative D), and for **2** (bottom), the magnetization is in the xy plane (positive D).

Table 3. Main perturbative contributions of the excited states to the D and E values for **2**.

	D [cm^{-1}]	E [cm^{-1}]
1st quartet	11.49	11.61
2nd quartet	13.07	−13.09
1st doublet	12.58	0

to the $\sum_i \hat{l}_i^+ \cdot \hat{s}_i^- + \hat{l}_i^- \cdot \hat{s}_i^+$ operators coupling the electron that is promoted from the d_{xz} or d_{yz} orbitals to the d_{z^2} orbital. The active spin–orbit operator in the present case couples M_S components differing by a value of 1. Thus, since the $M_S = 1/2$ (respectively $M_S = -1/2$) component of the ground quartet state interacts with both the $M_S = 3/2$ and $M_S = -1/2$ components (respectively $M_S = -3/2$ and $M_S = 1/2$) of the excited states, it benefits from two interactions, while the $M_S = 3/2$ and $M_S = -3/2$ ground state components only interact with the $M_S = 1/2$ or $M_S = -1/2$ components of the excited states, respectively. As a consequence the $M_S = \pm 1/2$ components of the quartet ground state are more stabilized than the $M_S = \pm 3/2$ state, and thus these excited states give a positive contribution to D (note that a positive D value means that the lowest absolute values of M_S are stabilized). The excited doublet state wave function is dominated by the $|d_{xy}\overline{d}_{xy}d_{z^2}|$ and $|d_{x^2-y^2}\overline{d}_{x^2-y^2}d_{z^2}|$ determinants, in which an

electron is promoted from the d_{xy} to the $d_{x^2-y^2}$ orbitals or from the $d_{x^2-y^2}$ to the d_{xy} orbital. The interactions therefore come from the $\sum \hat{l}_{zi} \cdot \hat{s}_{zi}$ operator and only the $M_S = \pm 1/2$ components of the ground state can be stabilized, while the $M_S = \pm 3/2$ state remains unaffected. This leads to an additional positive contribution to D. For Co^{II}, all the important contributions lead to stabilization of the $M_S = \pm 1/2$ components over the $M_S = \pm 3/2$ component, which is at the origin of the large positive D value for the Co^{II} complex. Because of the positive D value, the magnetization has an easy plane perpendicular to the $Co(H_2O)(NO_3)$ apical bonds (Figure 7, bottom).

Conclusion

The larger anisotropy found for Co^{II} in comparison to Ni^{II} is due to the fact that for the former all the excited states contribute to D in the same way (all positive), while for the latter the excited states have opposite contributions that reduce the overall D value. The difference in the sign of D stems mainly from the presence of a dominant negative contribution to D for Ni^{II}, while the contributions of all the excited states are positive for Co^{II}. It is interesting to see how the theoretical results can be used to tune and control the magnetic anisotropy in heptacoordinate Ni^{II} and Co^{II} complexes. Let us focus on Ni^{II}, which has negative and positive contributions to D. To increase the overall negative D value, one must 1) increase the effect of the coupling between the ground state and the first excited triplet by decreasing their energy difference and 2) decrease the effect of the coupling between the ground state and the higher excited triplets by increasing their energy difference. The first requirement can be achieved by reducing the energy difference between the $d_{x^2-y^2}$ and the d_{xy} orbitals by using a more symmetrical pentacoordinate ligand. The energy difference between the ground and the second and third excited triplet states can be increased by increasing the energy difference between the three sets of orbitals (d_{xz},d_{yz}), (d_{xy},$d_{x^2-y^2}$), and d_{z^2}, which will reduce the positive contribution to D and thus leads to a larger stabilization of the $M_S = \pm 1$ components. This can be achieved by substituting the axial ligands by a better σ donor to shift the d_{z^2} orbital upwards, and/or by a less effective π donor to shift the (d_{xz},d_{yz}) orbitals downwards. The same arguments hold for Co^{II}. To increase the positive D value, one must increase mainly the coupling with the first excited state by reducing its energy difference with the ground state. Replacing the apical ligands by weaker σ donors will reduce the energy difference between the (d_{xy}, $d_{x^2-y^2}$) and d_{z^2} orbitals and thus enhance the coupling and increase the positive D value.

This analysis allows a very simple qualitative evaluation tool to assess at least the sign of D for any electronic configuration of a 3d transition metal ion in a pentagonal-bipyramid surrounding to be proposed. For the high-spin d^6 configuration, the (d_{xz},d_{yz}) orbitals will have three electrons (see Figure 5). These two orbitals are both expressed as linear combinations of the d_{1+} and d_{1-} complex spherical harmonics. Electron promotion from d_{yz} to d_{xz}, which corresponds to the first excited triplet state, does not change the m_l values. Only the z component of the spin–orbit operator $\left(\sum_i \hat{l}_{zi} \cdot \hat{s}_{zi}\right)$ is therefore to be considered, as in the case of Ni^{II}, and a negative D value is expected. One of us has already reported a negative D value for a heptacoordinate pentagonal-bipyramidal high-spin Fe^{II} complex,[26] which confirms our prediction. The same kinds of arguments should allow prediction of a negative D value for the d^3 configuration (Cr^{III} and V^{II}), while a positive one is expected for the d^2 (V^{III}) and d^4 (Mn^{III}) configurations. Investigation of the magnetic anisotropy of such compounds is underway. However, when the states are strongly multiconfigurational and/or the excited states are quasidegenerate, the resulting sign of D is hard to predict from simple arguments.

Herein we have demonstrated that a combination of synthetic and theoretical approaches leads to a good understanding of the origin of the magnetic anisotropy in heptacoordinate Ni^{II} and Co^{II} complexes with a geometry close to pentagonal-bipyramidal. More importantly, it fills the gap between theory and experiment and opens the perspective of establishing a magnetostructural correlation for magnetic anisotropy that would allow chemists to tune and eventually control this important parameter in mononuclear complexes.

Experimental Section

Synthesis: Chemicals were purchased from Aldrich and used without further purification. 2,6-diacetylpyridinebis(benzoic acid hydrazone) (H_2DAPBH), $[Ni(H_2DAPBH)(H_2O)_2](NO_3)_2{\cdot}2H_2O$ (**1**) and $[Co(H_2DAPBH)(H_2O)(NO_3)](NO_3)$ (**2**) were synthesized according to literature procedures.[12] All solvents were from BDH and were used as received. All manipulations were conducted under standard benchtop conditions.

TGA of $[Ni(H_2DAPBH)(H_2O)_2](NO_3)_2{\cdot}2H_2O$: TGA was performed on a fresh crystalline sample of **1**, assumed to be $[Ni(H_2DAPBH)(H_2O)_2](NO_3)_2{\cdot}2H_2O$. The experiment was performed under a steady flow of air and the temperature increased at a rate of $5\,^{\circ}C\,min^{-1}$. The sample lost mass continuously, and at constant rate, from 40 to 110 °C. At this point it had lost approximately 8% of its original mass ($54\,g\,mol^{-1}$, or three molecules of water per mole). This species, postulated to be $\{Ni(H_2DAPBH)(H_2O)(NO_3)_2\}$, was stable up to 160 °C, at which point a dramatic loss of mass suggested thermolysis of the complex. The final uncharacterized material was a dark noncrystalline powder.

Magnetic measurements: Variable-temperature (300–2 K) magnetic data were measured on microcrystalline powdered samples of **1** and **2** in an eicosane matrix in 1.0 and 0.1 T fields with a Quantum Design MPMS5 SQUID magnetometer. The presence of eicosane precludes the loss of water molecules of crystallization when the sample is put under vacuum in the SQUID. The data were corrected for the diamagnetic contribution of the sample holder and eicosane and the diamagnetism of the sample estimated according to Pascal's constants. Low temperature (2, 4, and 6 K) variable-field (0–5 T) measurements were carried out in the same manner. The data were fitted by full diagonalization of the energy matrices for 120 orientations of each value of the magnetic field by means of a homemade program based on the following spin Hamiltonian: $\mathbf{H} = \mu_B \mathbf{S}\cdot\mathbf{g}\cdot\mathbf{B} + D[\mathbf{S}_z^2 - S(S+1)/3] + E[\mathbf{S}_x^2 - \mathbf{S}_y^2]$.

HF-HFEPR: EPR experiments were performed at the High Magnetic Field Laboratory, Grenoble, France. Ground crystals (approximately 50 mg) were pressed to form a pellet to reduce torquing under high magnetic fields. The simulation program is available from Dr. H. Weihe; for more information see http://sophus.kiku.dk/software/epr/epr.html.[14]

Computations: Experimental geometries were used for the present theoretical study. Calculations were performed using the two-step approach implemented in the ORCA code, in which the SOC and SSC relativistic effects are included a posteriori. First, several solutions of the nonrelativistic Born Oppenheimer Hamiltonian are calculated by complete active space self-consistent field (CASSCF) and post-CASSCF methods. Then, the state interaction matrix of the SOC and SSC between these different solutions is calculated and diagonalized. The Breit–Pauli SSC Hamiltonian and a mean-field SOC Hamiltonian are used. Dynamic correlation is introduced by using the *n*-electron valence second-order perturbation theory (NEVPT2) correlated energies in the diagonal elements of the SOC/SSC matrix while keeping the CASSCF wave functions. Def2-tzvpp basis set was used for the Ni and Co, Def2-tzvpp(-f) basis set for the O and N of the first coordination sphere, Def2-svp basis sets for C, and Def2-sv for H.

The $\overline{\overline{D}}$ tensor was extracted by using the effective Hamiltonian theory, which enables one to calculate numerically all the matrix elements of the anisotropic spin Hamiltonian from the ab initio energies and wave functions.

For the rationalization of the magnitude and sign of the ZFS parameters the $\overline{\overline{D}}$ tensor components were calculated using the perturbative method implemented in the ORCA code. These values are slightly overestimated in comparison to those obtained by using the effective Hamiltonian theory.

Acknowledgement

We thank the CNRS, the Université Paul Sabatier, the Université Paris Sud 11, the Spanish Ministry of Science and Innovation (Project No. CTQ2011-23140), and the Agence Nationale de la Recherche ANR (project TEMAMA ANR-09-BLAN-0195-01, CHIRnMAG ANR-09-BLAN-54-01) for financial support.

[1] D. Gatteschi, R. Sessoli, *Angew. Chem.* **2003**, *115*, 278; *Angew. Chem. Int. Ed.* **2003**, *42*, 268.
[2] A. Caneschi, D. Gatteschi, N. Lalioti, C. Sangregorio, R. Sessoli, G. Venturi, A. Vindigni, A. Rettori, M. G. Pini, M. A. Novak, *Angew. Chem.* **2001**, *113*, 1810; *Angew. Chem. Int. Ed.* **2001**, *40*, 1760.
[3] C. Coulon, H. Miyasaka, R. Clerac, *Struct. Bonding (Berlin)* **2006**, *122*, 163.
[4] R. Lescouëzec, J. Vaissermann, C. Ruiz-Perez, F. Lloret, R. Carrasco, M. Julve, M. Verdaguer, Y. Dromzee, D. Gatteschi, W. Wernsdorfer, *Angew. Chem.* **2003**, *115*, 1521; *Angew. Chem. Int. Ed.* **2003**, *42*, 1483.
[5] G. Rogez, J. N. Rebilly, A. L. Barra, L. Sorace, G. Blondin, N. Kirchner, M. Duran, J. van Slageren, S. Parsons, L. Ricard, A. Marvilliers, T. Mallah, *Angew. Chem.* **2005**, *117*, 1910; *Angew. Chem. Int. Ed.* **2005**, *44*, 1876.
[6] G. Charron, F. Bellot, F. Cisnetti, G. Pelosi, J. N. Rebilly, E. Riviere, A. L. Barra, T. Mallah, C. Policar, *Chem. Eur. J.* **2007**, *13*, 2774.
[7] J. N. Rebilly, G. Charron, E. Riviere, R. Guillot, A. L. Barra, M. D. Serrano, J. van Slageren, T. Mallah, *Chem. Eur. J.* **2008**, *14*, 1169.
[8] R. Maurice, R. Bastardis, C. de Graaf, N. Suaud, T. Mallah, N. Guihery, *J. Chem. Theory Comput.* **2009**, *5*, 2977.
[9] S. Petit, G. Pilet, D. Luneau, L. F. Chibotaru, L. Ungur, *Dalton Trans.* **2007**, 4582.
[10] L. F. Chibotaru, L. Ungur, C. Aronica, H. Elmoll, G. Pilet, D. Luneau, *J. Am. Chem. Soc.* **2008**, *130*, 12445.
[11] L. Ungur, L. F. Chibotaru, *J. Chem. Phys.* **2012**, *137*, 064112.
[12] T. J. Giordano, G. J. Palenik, R. C. Palenik, D. A. Sullivan, *Inorg. Chem.* **1979**, *18*, 2445.
[13] C. Pelizzi, G. Pelizzi, S. Porretta, F. Vitali, *Acta Crystallogr. Sect. A Acta Crystallogr. Sec. C* **1986**, *42*, 1131.
[14] C. J. H. Jacobsen, E. Pedersen, J. Villadsen, H. Weihe, *Inorg. Chem.* **1993**, *32*, 1216.
[15] R. Maurice, C. de Graaf, N. Guihery, *Phys. Rev. B* **2010**, *81*, 214427.
[16] R. Maurice, C. de Graaf, N. Guihery, *J. Chem. Phys.* **2010**, *133*, 084307.
[17] R. Maurice, N. Guihery, R. Bastardis, C. de Graaf, *J. Chem. Theory Comput.* **2010**, *6*, 55.
[18] R. Maurice, A. M. Pradipto, N. Guihery, R. Broer, C. de Graaf, *J. Chem. Theory Comput.* **2010**, *6*, 3092.
[19] R. Maurice, K. Sivalingam, D. Ganyushin, N. Guihery, C. de Graaf, F. Neese, *Inorg. Chem.* **2011**, *50*, 6229.
[20] C. Angeli, R. Cimiraglia, S. Evangelisti, T. Leininger, J. P. Malrieu, *J. Chem. Phys.* **2001**, *114*, 10252.
[21] D. Ganyushin, F. Neese, *J. Chem. Phys.* **2008**, *128*, 114117.
[22] N. Gilka, P. R. Taylor, C. M. Maria, *J. Chem. Phys.* **2008**, *129*, 044102.
[23] In the first one, the matrix of the spin–orbit and spin–spin couplings between all of the computed states is diagonalized and the effective Hamiltonian theory is used to extract the components of the $\overline{\overline{D}}$ tensor.[17] The second method is based on the quasidegenerate perturbation theory, in which the components of the tensor are calculated using perturbation theory. While less computationally demanding, it furnishes results in good agreement with the first method. Since it provides the different contributions of all the computed excited states to the *D* and *E* parameters, the second method is helpful for the rationalization of the magnitude and nature of the anisotropy.
[24] C. Duboc, D. Ganyushin, K. Sivalingam, M.-N. Collomb, F. Neese, *J. Phys. Chem. A* **2010**, *114*, 10750.
[25] F. Neese, ORCA—An Ab Initio, Density Functional and Semiempirical Program Package, version 2.6–35 (Germany).
[26] T. S. Venkatakrishnan, S. Sahoo, N. Brefuel, C. Duhayon, C. Paulsen, A. L. Barra, S. Ramasesha, J. P. Sutter, *J. Am. Chem. Soc.* **2010**, *132*, 6047.

Received: July 13, 2012
Published online: November 23, 2012

